Molecular Dynamics Used in Radiation Therapy

Qing Hou* and Yingguan Wang

Key Lab for Radiation Physics and Technology of Education Ministry of China, Institute of Nuclear Science and Technology, Sichuan University, Chengdu 610064, People's Republic of China

(Received 30 April 2001; published 26 September 2001)

In this Letter, classical molecular dynamics is used to deal with optimization problems occurring in intensity modulated radiation therapy. By introducing the concepts of virtual atom and virtual cluster, the optimization process in this kind of therapy can be considered as an analogy to finding the equilibrium configuration of a cluster. This viewpoint gives great insight into the optimization problems. To show how the idea works, a dose-based objective function is adopted to obtain the optimized intensity profiles. The results and high computational efficiency show that molecular dynamics is applicable clinically for this therapy. The idea presented here also could be inspiring to other fields where optimization problems exist.

DOI: 10.1103/PhysRevLett.87.168101 PACS numbers: 87.56.–v, 87.64.Aa

Methods or concepts developed in one area can sometimes be very useful in solving problems in other areas that have no relationship with the former at first glance. Classical molecular dynamics (CMD) is a powerful tool that has been widely applied in material science for a long time. Since there are many examples in the literature concerning the applications of CMD, we list only a few of them as examples [1–5]. For more complete introductions on CMD there are outstanding textbooks [6,7] that could be referred to. In the present Letter, we find for the first time that CMD can also be used for optimization problems in radiotherapy. Although we deal with only the optimization problems occurring in radiotherapy, we think the idea presented here could be inspiring to other fields where optimization problems exist.

In radiotherapy, the basic principle is to deliver a radiation dose to a tumor that is high enough to destroy the tumor while keeping the dose delivered to normal tissues as low as possible. Thus the treatment planning, that is a process by which physicians determine the radiation parameters according to anatomy information based on CT or other medical images of patients, is an indispensable part in radiotherapy [8]. In the last several years, the development of intensity modulated radiotherapy (IMRT), by which the intensities of rays are modulated across the beams (as shown in Fig. 1), makes it possible to generate a dose distribution that forms a high dose envelope closely matching the defined targets ([9–20], and references therein). Obviously, it is impossible to design the intensity profiles manually by the experience of physicians or clinical planners and thus an inverse treatment planning (ITP) is required. An ITP is to optimally design radiation parameters by given tumor and normal tissues and desirable dose distributions. This optimization process is performed by minimizing, probably along with certain constraints, an objective function $O(\mathbf{I}, \alpha)$, that is defined by biological or physical considerations where $\mathbf{I}$ is the intensity matrix and α is the matrix of other parameters involved. An essential constraint in this problem is I_i, the ith element of $\mathbf{I}$, is non-negative. Optimization algorithms that have been used for ITP can be classified grossly as stochastic and deterministic. Stochastic methods, such as the simulated annealing method [9,16] or genetic methods [20], are flexible and powerful methods but rarely are used clinically because they are too computer time consuming. Deterministic methods, such as gradient methods [11–14], and the iterative method [18,19], are efficient but they may suffer the problems of converging to a local minimum and giving unphysical solutions, e.g., I_i are negative.

In this paper, we show that the optimization problems in radiotherapy can be dealt with by classic molecular dynamics. In CMD, a simulated system starts from an initial configuration in phase space and then relaxes to an equilibrium state where the system has lowest free energy. The motions of atoms in the simulated system follow Newton's law. Considering a system of total potential V_T, the dynamics equation can be written

$$m_i \frac{d^2\mathbf{r}_i}{dt^2} = \mathbf{f}_i = -\nabla_{\mathbf{r}_i} V_T , \tag{1}$$

where $\mathbf{r}_i$ and $\mathbf{v}_i$ is the position and the velocity of atom i, respectively. m_i is the mass of the atom and $\mathbf{f}_i = -\nabla_{\mathbf{r}_i} V_T$ is the force on that atom. At zero temperature, the equilibrium state is the state of lowest potential and $\mathbf{f}_i$ is zero for all atoms. Comparing this process to the optimization process in ITP, we can make an analogy between $O(\mathbf{I}, \alpha)$ in radiotherapy and V_T in molecular dynamics. Furthermore, we can introduce the concept of virtual atoms by which the position and velocity of virtual atom i are I_i and $\upsilon_i = \frac{dI_i}{d\tau}$, respectively, where τ is a virtual time. The dynamics equation for virtual atoms i is thus read

$$M_i \frac{d^2 I_i}{d\tau^2} = -\frac{\partial O(\mathbf{I}, \alpha)}{\partial I_i} , \tag{2}$$

where M_i is the mass of atom i to be defined below according to characteristics of the objective function adopted.

The essential constraint $I_i \geq 0$ is analogous to a barrier of infinite height where the atoms are reflected, i.e., $v_i(\tau) = -v_i(\tau)$ when $I_i(\tau) \leq 0$. All the virtual atoms form a virtual cluster. A virtual cluster has its stable states because $O(\mathbf{I}, \alpha)$, as V_T, includes repelling and attracting components no matter what concrete form $O(\mathbf{I}, \alpha)$ takes. These two components come from the fact that a higher prescription dose on target requires increasing intensities, that means the atoms are repelled from $I = 0$, while a lower or zero prescription dose on normal tissues demands a decrease in the intensities. Compared to the simulated annealing method, the virtual atoms in CMD move following the dynamics equations, and thus the system reaches its equilibrium state faster (this is important in clinical applications) than the system in simulated annealing where the virtual atoms move randomly and make a lot of trial and error operations. Compared to gradient methods or steepest descent methods, because the virtual atoms have velocities, the virtual atoms can overcome the barrier and thus escape from the local minima.

Now we adopt a concrete objective function to show how the above idea works. There are many objective functions based on physical [9–20] or biological models ([21], for instance) that have been proposed. Biological objective functions can give directly a biological outcome, but they are still at a formation stage because of their empirical nature. Thus physical objective functions are most commonly used in clinical trials. Because it is beyond the aim of the present Letter to establish an objective function, we adopt here a traditional dose-based objective function that is the least square deviation of the prescription dose. Although various constraints on this objective function [12–14] have been proposed to limit the maximum dose that a normal tissue can receive or to improve the dose-volume behavior that is concerned in clinical trials, we consider only the essential constraint $I_i > 0$. Moreover, in some optimization processes with constraints, the optimization of objective here occurs as an intermediate step [12,19]. In the present viewpoint of CMD, we can handle efficiently the optimization problem with the constraints. We will present elsewhere results that deal with, in the present framework, optimization problems of constraints and with other kinds of objective functions.

The dose-based objective function is written in a discrete form:

$$O(\mathbf{I}, \alpha) = C \sum_{n=1}^{NV} w_n \left[\sum_{i=1}^{NP} I_i d_n^{(i)} - \overline{d}_n \right]^2, \qquad (3)$$

where $d_n^{(i)}$ is dose at voxel n contributed by ray i of one intensity unit, $\overline{d}_n$ is the prescription dose at voxel n, w_n is the weight factor that represents the importance of voxel n. NV and NP are the number of concerned voxels and number of rays, respectively. By Eqs. (2) and (3), the force on virtual atom j can be written

$$f_j = -\frac{\partial O(\mathbf{I}, \alpha)}{\partial I_j} = \sum_{i \neq j}^{NP} f_{ij} - I_j \sum_{i=1}^{NP} D_{ij} + \sum_{i=1}^{NP} \overline{D}_{ij}, \qquad (4)$$

where $f_{ij} = (I_j - I_i) D_{ij}$, $D_{ij} = \sum_{i=1}^{NP} w_n d_n^{(i)} d_n^{(j)}$, and $\overline{d}_n^{(i)} = (d_n^{(i)} \overline{d}_n / \sum_{i=1}^{NP} d_n^{(i)})$. By this equation, we have an interesting physical picture: atom j is connected by a spring of spring constant $\sum_{i=1}^{NP} D_{ij}$ to a center of infinite mass, and at the same time the atom is pulled away from the center by an external force $\sum_{i=1}^{NP} \overline{D}_{ij}$. The atom is connected also to other atoms by springs of spring constant D_{ij}, and the interaction between two atoms follows Newton's third law. D_{ij} represents actually the overlap between dose distributions of two rays. Obviously, for a given prescription dose, the intensities of two rays that have overlap dose distributions have competitions. Because $\sum_{i=1}^{NP} D_{ij}$ is much larger than D_{ij}, the movements of atoms can be thus divided into two components of high frequency and low frequency, respectively.

First, we neglect the low frequency component and consider high frequency component only. The oscillating period of the high frequency component is $\tau_j = \sqrt{M_j / \sum_{i=1}^{NP} D_{ij}}$. If we define the mass of atom j as

$$M_j = \sum_{i=1}^{NP} D_{ij}, \qquad (5)$$

then all atoms would oscillate with the same period and they reach their equilibrium position at the same time. In practice, we found that by this definition of atomic mass, the convergence is reached more quickly in calculations and the obtained intensity profiles have better smoothness. By Eq. (4), the equilibrium position for this component can be obtained analytically:

$$I_j^{(0)} = \frac{\sum_{i=1}^{NP} \overline{D}_{ij}}{\sum_{i=1}^{NP} D_{ij}}. \qquad (6)$$

This first order solution for the optimization problem is exact when there is no interaction between atoms, e.g., there is no overlap between dose distributions of two rays.

Because D_{ij} is much smaller than $\sum_{i=1}^{NP} D_{ij}$, the low frequency component is a relatively adiabatic movement. By Eqs. (2) and (4), we can apply any differential scheme used in CMD to obtain the movement trajectory of ray intensities. Here we apply the scheme of Swope *et al.* [22] that takes the form

$$I_j(\tau + \delta\tau) = I_j(\tau) + \delta\tau v_j(\tau) + \frac{1}{2M_j} \delta\tau^2 f_j(\tau), \qquad (7)$$

$$v_j(\tau + \delta\tau) = v_j(\tau) + \frac{1}{2M_j} \delta\tau [f_j(\tau) + f_j(\tau + \delta\tau)]. \qquad (8)$$

What should be mentioned is that $O(\mathbf{I}, \alpha)$ is a potential in the viewpoint of CMD. $O(\mathbf{I}, \alpha)$ is minimized when the

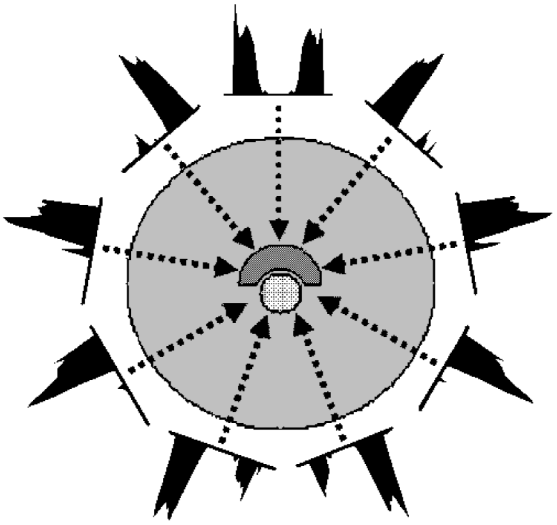

FIG. 1. A simulated IMRT example. The dark gray region is a simulated tumor, the light gray region is a simulated organ at risk (OAR), and the gray region is the normal tissue. Nine coplanar beams are applied to the target. Across the beams the intensities of rays are modulated. The intensity profiles are obtained by optimization algorithm given in the present Letter.

temperature is zero. Thus a damping scheme should be applied for cooling the system. The damping is included by multiplying velocity by a factor λ that is less than 1 when $v_j(\tau)f_j(\tau) < 0$. We found the value of λ has no obvious influence on the optimization results in the present paper while the influence can be observed if the volume constraint [14] is taken into account. We will discuss the problem elsewhere.

As a test of the present algorithm, we did the intensity optimization for an artificial sample shown in Fig. 1. The simulated phantom is a cylinder of radius of 15 cm. Located at the center of the phantom is a simulated tumor that is a half cylinder of radius of 4 cm. Close to the tumor is a simulated organ at risk (OAR) of 2 cm in radius. Nine coplanar beams of energy of 10 MeV are applied at equispaced entry angles. Because a discussion of the model for dose calculations is beyond the topic of the present Letter, the dose distribution of each ray is calculated by the exponential attenuation model of the primary beam without accounting for the scattering of photons in the phantom. Without considering any biological effects, we assign simply a prescription dose of 1 unit to the target and a prescription dose of 0 unit to OAR and normal tissues. The optimization starts at an initial intensity profile given by Eq. (6) and the mass of atoms is given by Eq. (5). Figure 2 shows the evolution of the objective function by time steps. The arrow points to where the non-negative constraints reflect the atoms. This is a feature not observed in usual gradient methods. Figures 3 and 4 show the Dose-Volume histogram and isodose curves, respectively. Obviously, the 80% isodose curve totally encloses the target very well while the dose in OAR is below the 40% level. In clinical applications, the computational efficiency is an important factor. In this example, the number of voxels is 53 715 and the number of rays is 1323. The calculation time was

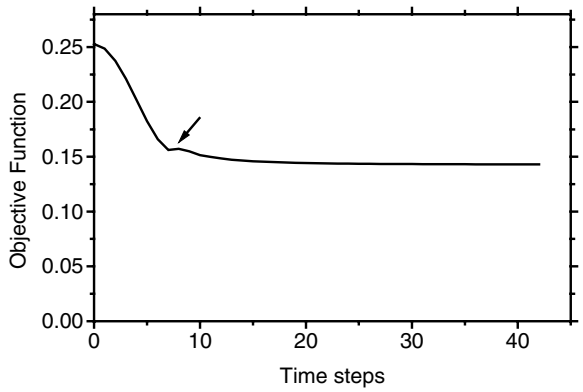

FIG. 2. Variation of objective function versus the time steps for example in Fig. 1. The arrow points to where the non-negative constraints reflect the atoms.

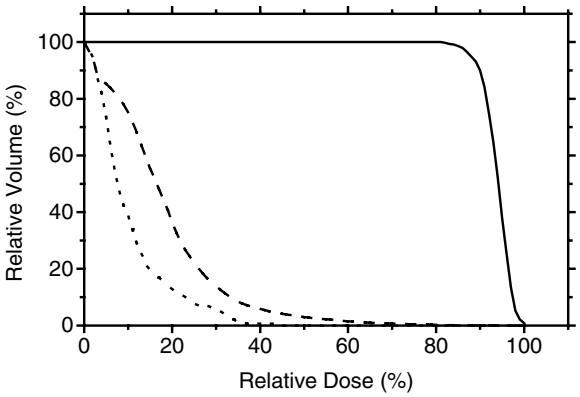

FIG. 3. Dose-volume histograms for the example in Fig. 1. Solid line: the tumor. Dotted line: the OAR. Dashed line: the normal tissue. Obviously, the whole tumor has a dose level above 80%. 95% volume of the tumor has a dose level above 90%. The dose level of OAR is well below 40%.

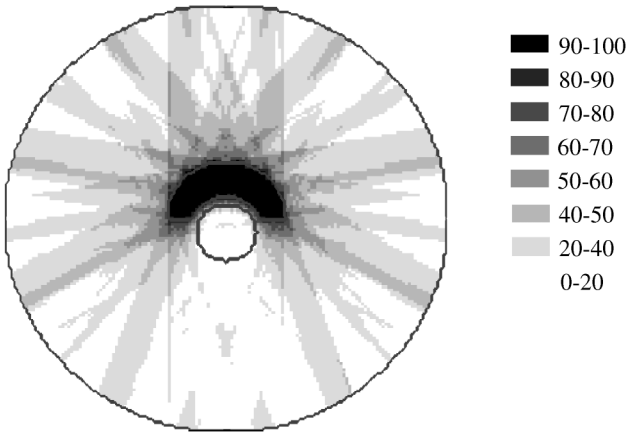

FIG. 4. Isodose curve for the example in Fig. 1. The 80% isodose curve completely encloses the tumor while the OAR is protected very well.

35 s on a PC Pentium III 500 mHz processor. Our other calculations with more voxels and rays included also show high computational efficiency. More complete results will be reported elsewhere.

In summary, we have presented a molecular dynamics viewpoint on the optimization problems in intensity modulated radiation therapy. By this viewpoint, the intensity optimization in IMRT can be considered to be equivalent to finding the equilibrium states of a cluster. Our testing examples show this idea is very useful in solving clinical problems. Another point we should emphasize is that the idea in the present Letter may not be limited to the application in radiotherapy, it presents a probable alternative way to solving optimization problems occurring in other fields.

This work is supported partly by the National Scientific Foundation of China (Contract No. 19875035) and Education Ministry of China. Qing Hou thanks Professor Marc Hou of Universite Libre de Bruxelles from whom Qing Hou learned a lot of techniques of molecular dynamics.

*Author to whom correspondence should be addressed. Electronic address: qhou@263.net or nic7602@scu.edu.cn

[1] J. Schiotz, F. D. Di Tolla, and K. W. Jacobsen, Nature (London) **39**, 561 (1998).
[2] L. J. Lewis, P. Jensen, and J.-L. Barrat, Phys. Rev. B **56**, 2248 (1997).
[3] W. D. Luedtke and Uzi Landman, Phys. Rev. Lett. **82**, 3835 (1999).
[4] Q. Hou, M. Hou, L. Bardotti, B. Prevel, P. Melinon, and A. Perez, Phys. Rev. B **62**, 2825 (2000).
[5] A. F. Voter, Phys. Rev. Lett. **78**, 3908 (1997).
[6] M. P. Allen and D. J. Tildesley, *Computer Simulation of Liquids* (Clarendon Press, Oxford, 1987).
[7] A. R. Leach, *Molecular Modelling* (Addison Wesley Longman Ltd., United Kingdom, 1996).
[8] S. Webb, *The Physics of Three-Dimensional Radiation Therapy* (IOP Publishing Ltd., Bristol, 1993).
[9] S. Webb, Phys. Med. Biol. **45**, 1715 (2000).
[10] Q. Wu, M. Arnfield, S. Tong, Y. Wu, and R. Mohan, Phys. Med. Biol. **45**, 1731 (2000).
[11] W. Laub, M. Albert, M. Birkner, and F. Nusslin, Phys. Med. Biol. **45**, 1741 (2000).
[12] R. Li and F. Yin, Med. Phys. **27**, 691 (2000).
[13] Q. Wu and R. Mohan, Med. Phys. **27**, 701 (2000).
[14] S. V. Spirou and Chen-Shou Chu, Med. Phys. **25**, 321 (1998).
[15] J. Llacer, Med. Phys. **24**, 1751 (1997).
[16] W. Webb, Phys. Med. Biol. **39**, 2229 (1994).
[17] P. S. Cho, S. Lee, R. J. Marks II, S. Oh, S. Sutlif, and M. H. Philips, Med. Phys. **25**, 435 (1998).
[18] X. Lei, R. J. Hamilton, D. Spelbring, C. A. Pelizzari, and G. T. Y. Chen, Med. Phys. **25**, 1858 (1999).
[19] X. Lei, J. G. Li, S. Donaldson, Q. T. Le, and A. L. Boyer, Phys. Med. Biol. **44**, 2525 (1999).
[20] G. A. Ezzell, Med. Phys. **23**, 293 (1996).
[21] M. Alber and F. Nusslin, Phys. Med. Biol. **44**, 479 (1999).
[22] W. C. Swope, H. C. Anderson, P. H. Berens, and K. R. Wilson, J. Chem. Phys. **76**, 1 (1982).